# Aqueous-phase synthesis of dual-anion CuInSeS quaternary quantum dots for ultrasensitive D-penicillamine detection via inter filter effect

Jing Chen[a], Dongjie Chen[a], Yuruo Zeng[a], Haiyan Zhong[a], Xinqi Zhang[b], Weiming Sun[a], Jinghua Chen[a] and Zhizhong Han[a,*]

[a]School of Pharmacy, Fujian Medical University, Fuzhou, Fujian 350122, China

[b]Fujian College Association Instrumental Analysis Center, Fuzhou University, Fuzhou, Fujian 350108, China

*Corresponding author:

E-mail: zzhan@fjmu.edu.cn (Z. Han)

## Experimental

### Reagents and instruments

Indium(III) acetate ($In(CH_3COO)_3$, 99.99%), sodium borohydride ($NaBH_4$, 99%), D-penicillamine (D-PA, ≥ 98%) were purchased from Shanghai Aladdin Bio-Chem Technology Co., Ltd (Shanghai, China). Sodium sulfide nonahydrate ($Na_2S·9H_2O$, ≥ 99.5%), zinc(II) acetate ($Zn(CH_3COO)_2$), copper(II) acetate monohydrate ($Cu(CH_3COO)_2·H_2O$), 3-mercaptopropionic acid (MPA, ≥ 99.5%), selenium powder (Se, 99.9%), iron(II) chloride ($FeCl_2$, 99.5%) were purchased from Shanghai Macklin Biochemical Co., Ltd (Shanghai, China).

The fluorescent spectra were recorded by a Lengguang F96Pro fluorescence spectrofluorometer (Shanghai, China). Fluorescence lifetime was collected by an Edinburgh FLS1000 spectrofluorometer. The ultraviolet-visible (UV-Vis) absorption spectra were obtained using a Thermo Fisher Scientific Gensys 150 spectrophotometer. The X-ray photoelectron spectroscopy (XPS) was taken with a Thermo Fisher Scientific K-Alpha+ X-ray photoelectron spectrometer. The Fourier transform infrared spectrum (FTIR) was recorded by a Thermo Fisher Scientific Nicolet IS50 Fourier infrared spectrometer.

1.2 Computational methods

All the density functional theory (DFT) calculations were performed by using the Gaussian 16 program.[1] Geometric optimization and frequency calculations have been performed at the PBE0/6-31+G(d)&LANL2DZ level. The binding energy (($E_b$) was calculated at the SMD-PBE0/def2TZVP level by considering the solvent effect of water via the solvation model based on density (SMD) [2] and dispersion correction of D3(BJ) [3]. The $E_b$ values of complexes were calculated by the following equation,

$$E_b = E(\mathrm{M}) + E(\text{D-PA}) - E(\text{complex})$$

## Results

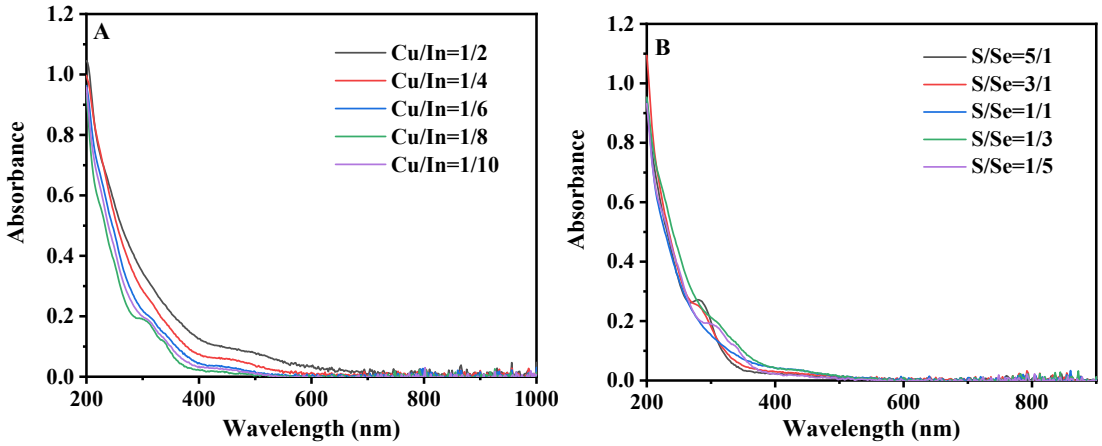


Fig. S1 (A) UV-Vis absorption spectra of CuInSeS QDs with different Cu/In ratios, (B) UV-Vis absorption spectra of CuInSeS QDs with different S/Se ratios

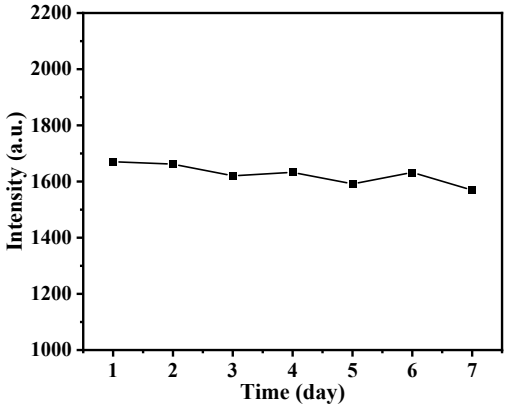


Fig. S2 The intensity of CuInSeS QDs for different days

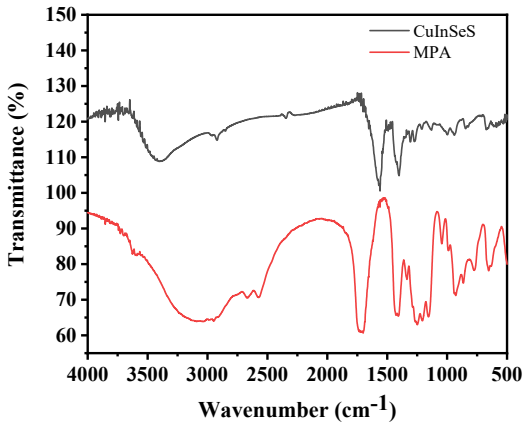


Fig. S3 FTIR spectra of CuInSeS QDs and MPA

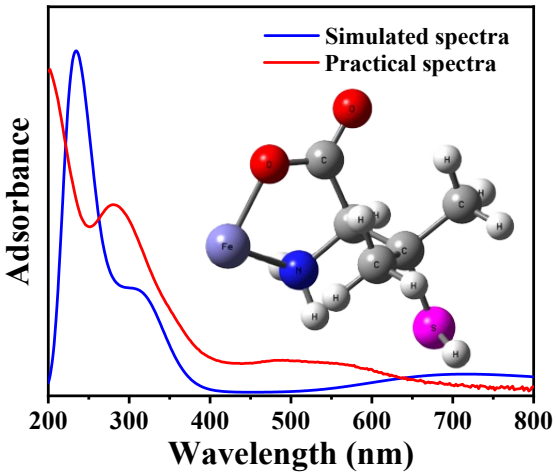


Fig. S4 The simulated and practical absorption spectra, the inset is the optimized geometric structure of complex with $Fe^{2+}$

Table S1 Comparison of the results of different materials used for the detection of D-PA

| **Materials** | **Linear range** | **LOD** | **Reference** |
|---|---|---|---|
| Au NCs-$Cu^{2+}$ | 1 ~ 10.5 μM | 0.08 μM | [4] |
| CDs-$Cu^{2+}$ | 0.1 ~ 1.0 and 1.0 ~ 50 μg/mL | 0.09 μg/mL | [5] |
| GQDs-$Pb^{2+}$ | 0.6 ~ 50 μM | 0.47 μM | [6] |
| CDs-$Hg^{2+}$ | 2 ~ 24 μM | 0.6 μM | [7] |
| SiQDs | 1 ~ 20 and 2 ~ 20 μM | 0.48 and 0.68 μM | [8] |
| AuAg@AuNPs | 0.0166 ~ 1.66 and 0.33 ~ 26.6 μg/mL | $6.64\times10^{-3}$ and 0.1 μg/mL | [9] |
| Cu-NC | 3.6 ~ 94 μM | 1.2 μM | [10] |
| CuInSeS-$Fe^{2+}$ | 18 ~ 1000 μM | 5.42 μM | This work |

Table S2 Binding energy ($E_b$) between $Fe^{2+}$ and D-PA of complex.

| Complexes | $E_b$ (kcal/mol) |
|---|---|
| $Fe^{2+}$+D-PA | 126.74 |

## References


1 M.J. Frisch, G.W. Trucks, H.B. Schlegel, G.E. Scuseria, M.A. Robb, J. R. Cheeseman, G. Scalmani, V. Barone, G.A. Petersson, H. Nakatsuji, X. Li, M. Caricato, A.V. Marenich, J. Bloino, B.G. Janesko, R. Gomperts, B. Mennucci, H.P. Hratchian, J.V. Ortiz, A.F. Izmaylov, J.L. Sonnenberg, Williams, F. Ding, F. Lipparini, F. Egidi, J. Goings, B. Peng, A. Petrone, T. Henderson, D. Ranasinghe, V.G. Zakrzewski, J. Gao, N. Rega, G. Zheng, W. Liang, M. Hada, M. Ehara, K. Toyota, R. Fukuda, J. Hasegawa, M. Ishida, T. Nakajima, Y. Honda, O. Kitao, H. Nakai, T. Vreven, K. Throssell, J.A. Montgomery Jr, J.E. Peralta, F. Ogliaro, M.J. Bearpark, J.J. Heyd, E.N. Brothers, K.N. Kudin, V.N. Staroverov, T.A. Keith, R. Kobayashi, J. Normand, K. Raghavachari, A.P. Rendell, J.C. Burant, S.S. Iyengar, J. Tomasi, M. Cossi, J.M. Millam, M. Klene, C. Adamo, R. Cammi, J.W. Ochterski, R.L. Martin, K. Morokuma, O. Farkas, J.B. Foresman and D.J. Fox, 2016 Gaussian 16 Rev. C.01, Wallingford, CT, Gaussian 16.

2 V.S. Bernales, A.V. Marenich, R. Contreras, C.J. Cramer and D.G. Truhlar, *J. Phys. Chem. B*, 2012, **116**, 9122-9129.

3 S. Grimme, S. Ehrlich and L. Goerigk, J. Comput. Chem., 2011, 32, 1456-1465.

4 Y.F. Chen, J. Qiao, Q.R. Liu, M.M. Zhang and L. Qi, *Anal. Chim. Acta*, 2018, **1026**, 133-139.

5 T. Naghdi, M. Atashi, H. Golmohammadi, I. Saeedi and M. Alanezhad, *J. Ind. Eng. Chem.*, 2017, 52, 162-167.

6 Q. Wang, L.F. Li, T.X. Wu, X.P. Kong, Q.G. Ma, C.L. Ma, *Spectrochim. Acta A*, 2020, **229**, 117924.

7 Y.S. Yuan, X. Zhao, S.P. Liu, Y.F. Li, Y. Shi, J.J. Yan and X.L. Hu, Sensor Actuat., B, 2016, **236**, 565-573.

8 J.Y. Liu, J.B. Zhang, M.K. Wang and X.G. Su, *Talanta*, 2021, **224**, 121886.

9 Z. Zhao, Y. Jiao, D.Z. Yang and Y.L. Yang, *Microchim. Acta*, 2024, **191**, 604.

10 X.P. Yang, X.Y. Xie, L. Jiang, Y.X. Fan, C.L. Zhang and Y. Wang, *Talanta*, 2025, 283, 127131.